Neuroadaptive Fault-Tolerant Control Under Multiple Objective Constraints With Applications to Tire Production Systems

Qian Cui, Yujuan Wang, and Yongduan Song, *Fellow, IEEE*

***Abstract*— Many manufacturing systems not only involve nonlinearities and nonvanishing disturbances but also are subject to actuation failures and multiple yet possibly conflicting objectives, making the underlying control problem interesting and challenging. In this article, we present a neuroadaptive fault-tolerant control solution capable of addressing those factors concurrently. To cope with the multiple objective constraints, we propose a method to accommodate these multiple objectives in such a way that they are all confined in certain range, distinguishing itself from the traditional method that seeks for a common optimum (which might not even exist due to the complicated and conflicting objective requirement) for all the objective functions. By introducing a novel barrier function, we convert the system under multiple constraints into one without constraints, allowing for the nonconstrained control algorithms to be derived accordingly. The system uncertainties and the unknown actuation failures are dealt with by using the deep-rooted information-based method. Furthermore, by utilizing a transformed signal as the initial filter input, we integrate dynamic surface control (DSC) into backstepping design to eliminate the feasibility conditions completely and avoid off-line parameter optimization. It is shown that, with the proposed neuroadaptive control scheme, not only stable system operation is maintained but also each objective function is confined within the prespecified region, which could be asymmetric and time-varying. The effectiveness of the algorithm is validated via simulation on speed regulation of extruding machine in tire production lines.**

***Index Terms*— Actuation failures, multiple objectives, neuroadaptive fault-tolerant control, process manufacturing systems.**

I. Introduction

MOST manufacturing and process systems normally operate under various constraints arising from security considerations, performance requirements, and/or physical limitations [1], [2]. For example, for robotic manipulators in the external environment [3]–[6], the position and velocity of the joint and end-effector are limited to certain safe range to avoid collision [7]–[9]. In the process of material transformation, the shortest distance traveled by the vehicle and the lowest transportation cost are multiobjective constraints [10]. The highest return, shortest cycle, and lowest risk are the multiple goals pursued by investors in investing an engineering project [11]. It is expected to achieve the goals of highest productivity, highest product purity with the lowest energy consumption in any manufacturing systems [12]. It should be noted that the aforementioned demands, such as increasing profits, reducing materials consumption, enhancing safety, and protecting the environment, would inevitably lead to multiple constrained objective functions, rendering the underlying control problem interesting yet challenging.

Much effort has been made in addressing the control problem of systems under constraints in the literature, such as model predictive control [13], reference governors [14], and extreme-seeking control [15]. More recently, several researchers have tackled the problem of controlling nonlinear systems involving constraints [16]–[19] based on the barrier Lyapunov function (BLF) or integral BLF, which is realized by using the fact that if a properly chosen BLF is ensured to be bounded, then its argument is bounded. It is noted that the feasibility conditions [20]–[22] on virtual controllers are imposed in most existing BLF-based methods for systems with full-state constraints, posing significant difficulty for controller design (parameter determination) and implementation. It should be noted that most existing constrained control methods can only deal with constraints that are directly imposed on system states or output [4], [6], [8], [9], [16], whereas in manufacturing systems, the constraints are normally imposed on a nonlinear combination of systems' states and output, calling for a more dedicated control solution.

As the feasibility conditions and accurate parameters are difficult to obtain, new control designs for the nonlinear systems under constraints that are independent of system parameters and feasibility conditions are highly desirable. In this article, our particular interest lies in control design that is independent of the feasibility conditions and demands little information on system parameters for a class of manufacturing systems involving not only nonvanishing uncertainties but also actuation failures and multiple yet possibly conflicting objectives.

Manuscript received October 4, 2019; revised December 3, 2019; accepted January 11, 2020. Date of publication February 17, 2020; date of current version August 4, 2021. This work was supported in part by the National Natural Science Foundation of China under Grant No. 61773081, No. 61860206008, No. 61803053, No. 61933012, No. 61833013, and No. 61991403. *(Corresponding author: Yongduan Song).*

The authors are with the Chongqing Key Laboratory of Intelligent Unmanned Systems, School of Automation, Chongqing University, Chongqing 400044, China (e-mail: qiancui@cqu.edu.cn; yjwang66@cqu.edu.cn; ydsong@cqu.edu.cn).

Color versions of one or more of the figures in this article are available online at https://ieeexplore.ieee.org.

Digital Object Identifier 10.1109/TNNLS.2020.2967150

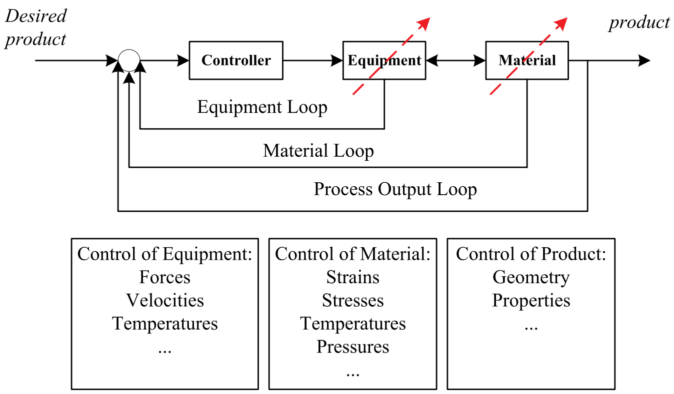

Fig. 1. Block diagram of control of manufacturing systems.

It is noted that the controller design and stability analysis for such systems is nontrivial because the process manufacturing systems are highly nonlinear and strongly coupled. The underlying control problem becomes even more challenging when multiple objectives are involved, as usually in practice, such as maximizing quality [23], improving throughput [24], [25], increasing flexibility [26], [27], and reducing cost [28], [29], as conceptually shown in Fig. 1.

In this article, we propose a neuroadaptive fault-tolerant control scheme for such manufacturing systems under multiple objective constraints. Compared with the existing results, the main features and contributions of the proposed method can be summarized as follows.

1) The system considered in this article is subject to not only unknown actuation failures but also multiple objective constraints, both of which make the control problem of such system much interesting yet challenging. This article provides a systemic strategy to address the control problem for such systems, which has rarely been reported in the existing studies.
2) By introducing appropriate weighting coefficients in objective functions, the multiple objective constraints are accommodated in such a way that they are all confined in certain acceptable range, circumventing the complicated procedure to search for a common optimum for all the objective functions that might not even exist due to the complicated and conflicting objective requirements.
3) A different coordination is introduced to start the dynamic surface control (DSC)-based backstepping design, which not only completely eliminates the feasibility conditions but also removes the process of off-line parameter optimization.
4) The system uncertainties and actuation failures are estimated by the so-called deep-rooted information-based approximation method, and the other unknown factors are approximated by neural networks (NNs). By skillfully combining the two approximation methods, all the uncertain factors in the system considered in this article are handled gracefully.

II. Problem Formulation

To reflect the fact that most manufacturing systems not only involve nonlinearities and nonvanishing disturbances but also are subject to actuation faults and multiple objectives, we consider the following dynamic systems:

$$\begin{cases} \dot{x}_k = b_k(\bar{x}_k)x_{k+1} + f_k(\bar{x}_k) + d_k(t), \qquad k = 1, \dots, n-1 \\ \dot{x}_n = b_n(\bar{x}_n)u + f_n(\bar{x}_n) + d_n(t) \\ y = x_1 \end{cases} \tag{1}$$

under loss-of-effectiveness actuation faults

$$u = \varrho(t_\varrho, t)u_d + \vartheta(t - t_f)\sigma_d(t) \tag{2}$$

and subject to multiple objective constraints

$$\begin{aligned} G_1 &= \min\{\xi_1\} \\ G_2 &= \max\{\xi_2\} \\ &\vdots \\ G_m &= \max\{\xi_m\} \end{aligned} \tag{3}$$

with $m \geq 2$. Note that G_1 represents the minimum optimization value, which may serve as the lowest production cost with ξ_1 being the cost function. G_2 denotes the maximum optimization value, which can serve as the highest production rate with ξ_2 being the rate function. G_3 to G_m bear similar physical meaning.

However, considering that the multiple objectives may be contradictory, it is impractical to make all objective functions be optimal at the same time in a real-time environment. How to come up with a compromised solution so that the objective functions approach to the optimal solution [which can be denoted by following inequalities (4)], is what we concentrate on:

$$\begin{aligned} F_{11}(t) &< J_1(x_1) < F_{12}(t) \\ F_{21}(t) &< J_2(x_1) < F_{22}(t) \\ &\vdots \\ F_{m1}(t) &< J_m(x_1) < F_{m2}(t) \end{aligned} \tag{4}$$

$$J_i = \omega_1 x_1 + \omega_2 x_1^2 + \cdots \omega_i x_1^i. \tag{5}$$

By introducing the weighting coefficients ω_i contained in J_i, $i = 1, 2, \dots, m$ the upper and lower bounds of J_i can be unified in the same boundary, which can be described specifically as

$$F_1(t) < \{J_1(x_1), J_2(x_1), \dots, J_m(x_1)\} < F_2(t) \tag{6}$$

with

$$\begin{aligned} F_1(t) &= \max\{F_{11}(t), F_{21}(t), \dots, F_{m1}(t)\} \\ F_2(t) &= \min\{F_{12}(t), F_{22}(t), \dots, F_{m2}(t)\}. \end{aligned} \tag{7}$$

Note that in (1), $\overline{x}_k = [x_1, \dots, x_k]^T \in \mathbb{R}^k (k = 1, \dots, n)$ denotes the system state vector, $u \in \mathbb{R}$ and $y \in \mathbb{R}$ denote the control input and output, respectively, $b_k(\cdot)(k = 1, \dots, n)$ denotes the control gain, $f_k(\cdot)$ denotes unknown nonlinear uncertainty, and $d_k(t)$ denotes unknown continuous external disturbance.

In the system model (1), modeling uncertainties and nonlinearities, external disturbances, and objective function constraints are taken into consideration at the same time.

In addition, actuation failures may arise from process manufacturing, leading to the actual control input u being not in accordance with the desired control input u_d, such as (2). In (2), $\varrho(t_\varrho, t)$ denotes the "healthy indicator" reflecting the actuation effectiveness, $\vartheta(t-t_f)\sigma_d(t)$ denotes uncontrollable actuation fault, and t_ϱ and t_f represent the time instants at which the actuation losses the effectiveness and actuation fault takes action, respectively. In this article, the case is considered that the actuator suffers from losing actuation effectiveness in that $0 < \varrho \leq 1$. Note that the actuator will not fail to function if $\varrho = 1$. Denote the minimum value of ϱ as $\varrho_{\min}$.

In (6), $J_i(x_1)$ represents the ith $(i = 1, 2, \ldots, m)$ objective function, $F_1(t)$ and $F_2(t)$ denote the asymmetric and possibly time-varying lower and upper bounds, respectively. $J(x_1)$ is the abstract function depending on x_1 and satisfying condition $(\partial J(x_1))/(\partial x_1) \neq 0$. It is worth mentioning that the multiple objective functions can be bounded within the same constraints by setting the coefficients ω_i $(i = 1, \ldots, m)$ properly in the objective function while satisfying the aforementioned partial derivative condition.

Remark 1: It should be pointed out that $J = x_1$ corresponds to output constraints issue, which has attracted considerable attention, such as [8], [30]–[32]. However, to the best of our knowledge, there is still no result investing various combinations of output x_1.

The control objective is to design a control scheme for nonlinear system (1) such that the following holds.

1) The asymmetric objective function constraints are never violated.
2) The feasibility conditions are completely removed.
3) All closed-loop signals are guaranteed bounded.

To this end, the following assumptions are necessary.

Assumption 1 ([33], [34]): The sign of $b_k(\overline{x}_k)$ $(k = 1, \ldots, n)$ is positive definite and there exists unknown positive constant $\underline{b}_k$ and $\overline{b}_k$ satisfying $0 < \underline{b}_k \leq b_k(\cdot) \leq \overline{b}_k < \infty$.

Assumption 2 ([8]): There exists some unknown positive constant ν_m such that $|\vartheta(t-t_f)\sigma_d(t)| \leq \nu_m < \infty$.

Assumption 3 ([35]): Assume that for unknown nonlinear function $f_k(\bar{x}_k)$ $(k = 1, \ldots, n)$, there exist unknown constant a_k and known smooth function $\varphi_k(\bar{x}_k)$ such that $|f_k(\bar{x}_k)| \leq a_k\varphi_k(\bar{x}_k)$, where $\varphi_k(\bar{x}_k)$ is bounded if $\bar{x}_k$ is bounded.

Here, in this article, the radial basis function NNs (RBFNNs), as shown in Fig. 2, are applied to approximate some unknown and continuous functions. According to [36]–[38], for any given continuous function $\psi(Z)$ on a compact set Ω_Z, the following relation holds:

$$\psi(Z) = W^{*T} S(Z) + \delta(Z) \tag{8}$$

where W^{*T} denotes the optimal constant weight, $\delta(Z)$ denotes the approximation error, and $S(Z) = [S_1(Z), \ldots, S_p(Z)]^T$ is the basis function vector with p representing the number of neurons. Commonly chosen Gaussian function is assigned to $S_i(Z)$ with the form

$$S_i(Z) = \exp\left(-\frac{(Z-\omega_i)^T(Z-\omega_i))}{\phi_i^2}\right) \tag{9}$$

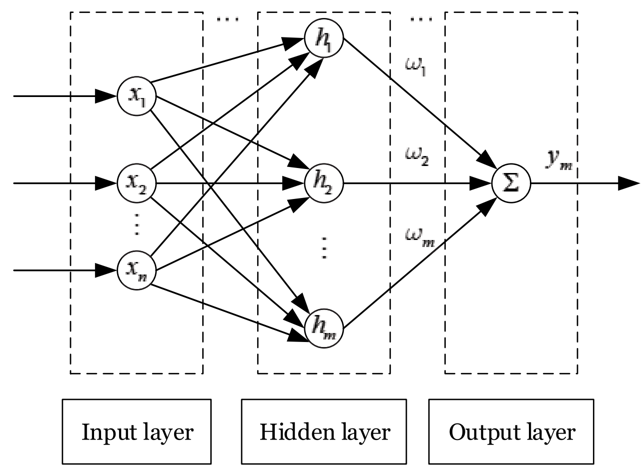

Fig. 2. Schematic of NN.

where $\omega_i = [\omega_{i1}, \ldots, \omega_{iq}]^T$ $(i = 1, \ldots, p)$ denotes the center of receptive field and ϕ_i is the width of the Gaussian function. For all $Z \in \Omega_Z$, W^* satisfies

$$W^* = \arg\min_{W \in \mathbb{R}^p} (\sup |W^T S(Z) - \psi(Z)|). \tag{10}$$

Generally, the choice of RBFNN obeys following guidelines [39].

1) The approximation error $\delta(Z)$ can be decreased by increasing the numbers of neuron properly.
2) The center of receptive field ω_i evenly covers the NN approximation region.
3) The width of the Gaussian function ϕ_i can be obtained from $\phi_i = \sqrt{2}d_{\max}/\sqrt{p}$ with $d_{\max}$ being the maximal Euclid distance of the approximation region.
4) The approximation error $\delta(Z)$ can be confined in a compact set Ω_z if ω_i and ϕ_i are chosen appropriately and p is sufficiently large [40], [41].

Based on the universal approximation theorem, it can be inferred that if the NN node p is large enough, $\delta(Z)$ can be bounded by an arbitrarily small value, i.e., $\delta(Z) \leq \epsilon < \infty$ with $\epsilon > 0$. In this article, in order to simplify the online computation, a virtual parameter is introduced

$$\theta = \max\{\|W_i^*\|^2, i = 1, \ldots, n\}. \tag{11}$$

Since W_i^* is unknown, so is θ. The purpose of introducing the virtual parameter θ as defined in (11) is to avoid updating every weight of each layer at every sampling cycle, significantly reducing the computation burden as seen in the sequel.

The detail of the control development and its verification are presented in what follows.

III. Neuroadaptive Tracking Control Under Objective Constraints

To facilitate control design, we introduce the following barrier function first.

A. Barrier Function

To deal with dynamic constraints gracefully, a novel barrier function [42] is introduced.

The barrier function is constructed as

$$\zeta = \frac{J - \overline{F}_1}{J - F_1} + \frac{J - \underline{F}_2}{F_2 - J} \tag{12}$$

which is well defined in the open region Ω with the initial value located in the region, i.e., $J(0) \in \Omega$, and J is an abstract function with respect to x_1. There exist the upper and lower bounds $\overline{F}_1$ and $\underline{F}_2$ such that $F_1 < \overline{F}_1$ and $F_2 > \underline{F}_2$.

Remark 2: For any initial value $J(0) \in \Omega$, $\zeta \to \infty$ if $J \to F_1^+(t)$ or $J \to F_2^-(t)$. In other words, for any initial value $J(0) \in \Omega$, J can obey the asymmetric constraints as long as ζ is guaranteed bounded. Thus, the issue of making the objective function satisfy asymmetric constraints can be transformed into ensuring the boundedness of ζ.

From (12), it follows:

$$\zeta = \zeta_1 J + \zeta_2 \tag{13}$$

with

$$\begin{aligned} \zeta_1 &= \frac{\overline{F}_1 - F_1 + F_2 - \underline{F}_2}{(J - F_1)(F_2 - J)} \\ \zeta_2 &= \frac{F_1 \underline{F}_2 - \overline{F}_1 F_2}{(J - F_1)(F_2 - J)} \end{aligned} \tag{14}$$

which are well defined in Ω.

Thus, it can be obtained

$$J = \frac{\zeta}{\zeta_1} - \zeta_3 \tag{15}$$

where ζ_3 is defined as

$$\zeta_3 = \frac{\zeta_2}{\zeta_1} = \frac{F_1 \underline{F}_2 - \overline{F}_1 F_2}{\overline{F}_1 - F_1 + F_2 - \underline{F}_2} \tag{16}$$

which are well defined in Ω.

Taking the derivative of ζ, it yields

$$\dot{\zeta} = \eta_1 \dot{J} + \eta_2 \tag{17}$$

with

$$\begin{aligned} \eta_1 &= \frac{\overline{F}_1 - F_1}{(J - F_1)^2} + \frac{F_2 - \underline{F}_2}{(F_2 - J)^2} \\ \eta_2 &= \frac{(J - \overline{F}_1)\dot{F}_1}{(J - F_1)^2} - \frac{(J - \underline{F}_2)\dot{F}_2}{(F_2 - J)^2}. \end{aligned} \tag{18}$$

Equation (17) can be rewritten as

$$\dot{\zeta} = \eta_1 \frac{\partial J}{\partial x_1} \dot{x}_1 + \eta_2 \tag{19}$$

$$\dot{\zeta} = \eta_{11} \dot{x}_1 + \eta_2 \tag{20}$$

where $\eta_{11} = \eta_1 (\partial J / \partial x_1)$. From (18) and $(\partial J / \partial x_1) \neq 0$, it implies that $\eta_{11} \neq 0$.

B. Controller Design

The controller design is implemented by means of DSC and backstepping technologies. For convenience of later stability analysis, some auxiliary variables are defined

$$z_1 = \zeta_1 - \alpha_{1f} \tag{21}$$

$$z_k = x_k - \alpha_{kf}, \quad k = 2, \ldots, n \tag{22}$$

where z_k $(k = 1, \ldots, n)$ is the virtual error, α_{1f} is defined

$$\alpha_{1f} = \frac{J(y_d) - \overline{F}_1}{J(y_d) - F_1} + \frac{J(y_d) - \underline{F}_2}{F_2 - J(y_d)}. \tag{23}$$

Suppose that the derivatives up to second order of the desired trajectory y_d are known and bounded, there exist the upper and lower bounds of y_d, i.e., $\overline{y}_d$ and $\underline{y}_d$ such that $J(\underline{y}_d) - F_1 > 0$ and $F_2 - J(\overline{y}_d) > 0$. Then, it turns out that α_{1f} is bounded and well defined.

α_{kf} and α_{k-1} with $k = 2, \ldots, n$ are contained in following first-order filter:

$$\tau_k \dot{\alpha}_{kf} + \alpha_{kf} = \alpha_{k-1}, \qquad k = 2, \ldots, n \tag{24}$$

with α_{k-1} being the inputs serving as the virtual control simultaneously, α_{kf} being the outputs, and τ_k being positive constant assigned by the designer.

The filter error is defined as

$$y_k = \alpha_{kf} - \alpha_{k-1}, \quad k = 2, \ldots, n. \tag{25}$$

From (22) and (25), it turns out

$$x_k = z_k + y_k + \alpha_{k-1}, \quad k = 2, \ldots, n. \tag{26}$$

Define virtual parameters λ_k

$$\lambda_k = \max\left\{1, a_k^2, \frac{\overline{b}_k^2}{\underline{b}_k}\right\}, \quad k = 1, \ldots, n. \tag{27}$$

Next, the controller design is carried out step by step.

Step 1: Note that $z_1 = \zeta - \alpha_{1f}$, then it follows:

$$\begin{aligned} \dot{z}_1 &= \eta_{11} \dot{x}_1 + \eta_2 - \dot{\alpha}_{1f} \\ &= \eta_{11}(b_1 x_2 + f_1 + d_1) + \eta_2 - \dot{\alpha}_{1f}. \end{aligned} \tag{28}$$

Because of its universal approximation capability, NN shows excellent performance in dealing with modeling uncertainties and coupling nonlinearities in nonlinear system control designs [6], [43]. Many NN-based controllers depend on multilayer feedforward NN or RBFNNs. These feedforward architectures bear a static input-to-output map structure that requires a large number of neurons to represent the complex nonlinear systems. Therefore, the output is determined by the present input of the NN. Based on the characteristics of NN, it is adopted to approximate the unknown nonlinear term containing unknown disturbances.

By employing the RBFNN, it can be obtained

$$\begin{aligned} z_1 \dot{z}_1 &= z_1 \eta_{11}(b_1 x_2 + f_1 + d_1) + z_1 \eta_2 - z_1 \dot{\alpha}_{1f} \\ &= z_1 \eta_{11} b_1 (z_2 + y_2 + \alpha_1) + z_1 \eta_{11} f_1 + z_1 \eta_{11} d_1 \\ &\quad + z_1 \eta_2 - z_1 \dot{\alpha}_{1f} \\ &= z_1 \eta_{11} b_1 \alpha_1 + \Pi_1 + \Xi_1 \\ &= z_1 \eta_{11} b_1 \alpha_1 + \Pi_1 + z_1 \left(W_1^{*T} S_1 + \delta_1\right) \end{aligned} \tag{29}$$

where $\Pi_1 = z_1 \eta_{11} b_1 z_2 + z_1 \eta_{11} b_1 y_2 + z_1 \eta_{11} f_1$ and $\Xi_1 = z_1 \Lambda_1$, with $\Lambda_1 = \eta_{11} d_1 + \eta_2 - \dot{\alpha}_{1f}$ being continuous nonlinear function.

Based on Assumption 3 and Young inequality, it yields

$$b_1 \eta_{11} z_1 z_2 \le \varrho_{\min} \underline{b}_2 \eta_{11}^2 z_1^2 z_2^2 + \frac{\overline{b}_1^2}{4 \varrho_{\min} \underline{b}_2} \tag{30}$$

$$b_1\eta_{11}z_1 y_2 \le \varrho_{\min}\underline{b}_1\frac{\overline{b}_1^2}{\underline{b}_1}\eta_{11}^2 z_1^2 + \frac{y_2^2}{4\varrho_{\min}} \tag{31}$$

$$\eta_{11}z_1 f_1 \le \varrho_{\min}\underline{b}_1 a_1^2\varphi_1^2\eta_{11}^2 z_1^2 + \frac{1}{4\varrho_{\min}\underline{b}_1} \tag{32}$$

$$z_1 W_1^{*T}S_1 \le \varrho_{\min}\theta\underline{b}_1 S_1^2 z_1^2 + \frac{1}{4\varrho_{\min}\underline{b}_1} \tag{33}$$

$$z_1\delta_1 \le \varrho_{\min}\underline{b}_1 z_1^2 + \frac{\epsilon^2}{4\varrho_{\min}\underline{b}_1}. \tag{34}$$

According to the above-mentioned inequalities and (27) for $k=1$, it can be obtained as

$$\begin{aligned}\Pi_1 + \Xi_1 &\le \varrho_{\min}\underline{b}_1\lambda_1 z_1^2\big(\eta_{11}^2+\eta_{11}^2\varphi_1^2+1\big) + \varrho_{\min}\theta\underline{b}_1 S_1^2 z_1^2 \\ &\quad + \varrho_{\min}\underline{b}_2\eta_{11}^2 z_1^2 z_2^2 + \frac{y_2^2}{4\varrho_{\min}} + \frac{\overline{b}_1}{4\varrho_{\min}\underline{b}_2} + \frac{1}{2\varrho_{\min}\underline{b}_1} + \frac{\epsilon^2}{4\varrho_{\min}\underline{b}_1} \\ &\le \varrho_{\min}\underline{b}_1\lambda_1 z_1^2\Phi_1 + \varrho_{\min}\theta\underline{b}_1 S_1^2 z_1^2 + \varrho_{\min}\underline{b}_2\eta_{11}^2 z_1^2 z_2^2 \\ &\quad + \frac{y_2^2}{4\varrho_{\min}} + \Delta_1\end{aligned} \tag{35}$$

with $\Phi_1 = \eta_{11}^2 + \eta_{11}^2\varphi_1^2 + 1$, $\Delta_1 = (\overline{b}_1)/(4\varrho_{\min}\underline{b}_2) + (1)/(2\varrho_{\min}\underline{b}_1) + (\epsilon^2)/(4\varrho_{\min}\underline{b}_1)$.

Therefore

$$\begin{aligned}z_1\dot{z}_1 &\le b_1\eta_{11}z_1\alpha_1 + \varrho_{\min}\underline{b}_1\lambda_1 z_1^2\Phi_1 \\ &\quad + \varrho_{\min}\theta\underline{b}_1 S_1^2 z_1^2 + \varrho_{\min}\underline{b}_2\eta_{11}^2 z_1^2 z_2^2 + \frac{y_2^2}{4\varrho_{\min}} + \Delta_1.\end{aligned} \tag{36}$$

Define the Lyapunov candidate function

$$V_1 = \frac{1}{2}z_1^2 + \frac{\varrho_{\min}\underline{b}_1}{2\gamma_1}\tilde{\lambda}_1^2 + \frac{1}{2}y_2^2 \tag{37}$$

where $\gamma_1 > 0$ is a design parameter and $\tilde{\lambda}_1 = \lambda_1 - \hat{\lambda}_1$ is the virtual parameter estimate error with $\hat{\lambda}_1$ being the parameter estimate of λ_1.

By utilizing (36), the time derivative of V_1 is computed as

$$\begin{aligned}\dot{V}_1 &= z_1\dot{z}_1 + \frac{\varrho_{\min}\underline{b}_1}{\gamma_1}\tilde{\lambda}_1\dot{\tilde{\lambda}}_1 + y_2\dot{y}_2 \\ &\le b_1\eta_{11}z_1\alpha_1 + \varrho_{\min}\underline{b}_1\lambda_1 z_1^2\Phi_1 + \varrho_{\min}\theta\underline{b}_1 S_1^2 z_1^2 \\ &\quad + \varrho_{\min}\underline{b}_2\eta_{11}^2 z_1^2 z_2^2 + \frac{y_2^2}{4\varrho_{\min}} + \Delta_1 - \frac{\varrho_{\min}\underline{b}_1}{\gamma_1}\tilde{\lambda}_1\dot{\hat{\lambda}}_1 + y_2\dot{y}_2.\end{aligned} \tag{38}$$

The virtual control and adaptive control law are designed as

$$\alpha_1 = -\frac{1}{\eta_{11}}\big(c_1 z_1 + \hat{\lambda}_1 z_1\Phi_1 - \hat{\theta}S_1^2 z_1\big) \tag{39}$$

$$\dot{\hat{\lambda}}_1 = \gamma_1 z_1^2\Phi_1^2 - \mu_1\hat{\lambda}_1 \tag{40}$$

where c_1, γ_1, and μ_1 are positive design parameters and $\hat{\theta}$ is the estimation of θ with $\hat{\theta} = \theta - \tilde{\theta}$.

Based on the definition of y_2, it follows $\dot{y}_2 = \dot{\alpha}_{2f} - \dot{\alpha}_1 = -(y_2/\tau_2) - \dot{\alpha}_1 = -(y_2/\tau_2) + \Gamma_1(\cdot)$ with $\Gamma_1(\overline{z}_3, \overline{y}_3, \overline{\hat{\lambda}}_2, \overline{\hat{\theta}}_2, \ddot{\overline{y}}_d) = -((\partial\alpha_1/\partial\eta_{11})\dot{\eta}_{11} + (\partial\alpha_1/\partial z_1)\dot{z}_1 + (\partial\alpha_1/\partial\hat{\lambda}_1)\dot{\hat{\lambda}}_1 + (\partial\alpha_1/\partial\Phi_1)\dot{\Phi}_1)$ being a continuous function. Then, it yields

$$\begin{aligned}y_2\dot{y}_2 &= -\frac{y_2^2}{\tau_2} + y_2\Gamma_1 \\ &\le \left(\frac{1}{4} - \frac{1}{\tau_2}\right)y_2^2 + \Gamma_1^2.\end{aligned} \tag{41}$$

Based on (39)–(41), (38) can be reexpressed

$$\begin{aligned}\dot{V}_1 &\le -b_1c_1z_1^2 - b_1\hat{\lambda}_1 z_1^2\Phi_1 - b_1\hat{\theta}S_1^2 z_1^2 + \varrho_{\min}\underline{b}_1\lambda_1 z_1^2\Phi_1 \\ &\quad + \varrho_{\min}\theta\underline{b}_1 S_1^2 z_1^2 + \varrho_{\min}\underline{b}_2\eta_{11}^2 z_1^2 z_2^2 + \frac{y_2^2}{4\varrho_{\min}} + \Delta_1 \\ &\quad - \varrho_{\min}\underline{b}_1\tilde{\lambda}_1 z_1^2\Phi_1 + \frac{\varrho_{\min}\underline{b}_1\mu_1}{\gamma_1}\tilde{\lambda}_1\hat{\lambda}_1 + \left(\frac{1}{4} - \frac{1}{\tau_2}\right)y_2^2 + \Gamma_1^2 \\ &\le -\underline{b}_1c_1z_1^2 - \varrho_{\min}\underline{b}_1\hat{\lambda}_1 z_1^2\Phi_1 - \varrho_{\min}\underline{b}_1\hat{\theta}S_1^2 z_1^2 \\ &\quad + \varrho_{\min}\underline{b}_1\lambda_1 z_1^2\Phi_1 + \varrho_{\min}\theta\underline{b}_1 S_1^2 z_1^2 + \varrho_{\min}\underline{b}_2\eta_{11}^2 z_1^2 z_2^2 \\ &\quad + \frac{y_2^2}{4\varrho_{\min}} + \Delta_1 - \varrho_{\min}\underline{b}_1\tilde{\lambda}_1 z_1^2\Phi_1 + \frac{\varrho_{\min}\underline{b}_1\mu_1}{\gamma_1}\tilde{\lambda}_1\hat{\lambda}_1 \\ &\quad + \left(\frac{1}{4} - \frac{1}{\tau_2}\right)y_2^2 + \Gamma_1^2 \\ &\le -b_1c_1z_1^2 - \varepsilon_2^* y_2^2 - \frac{\varrho_{\min}\underline{b}_1\mu_1}{2\gamma_1}\tilde{\lambda}_1^2 + \varrho_{\min}\underline{b}_1\tilde{\theta}S_1^2 z_1^2 \\ &\quad + \varrho_{\min}\underline{b}_2\eta_{11}^2 z_1^2 z_2^2 + \Gamma_1^2 + \omega_1\end{aligned} \tag{42}$$

with $-b_1 < -b_1\varrho_{\min} \le -\underline{b}_1\varrho_{\min}$, $\omega_1 = \Delta_1 + (\varrho_{\min}\underline{b}_1\mu_1)/(2\gamma_1)\lambda_1^2$, and $\varepsilon_2^* \ge (1/\tau_2) - (1/4) - (1/4\varrho_{\min})$ being arbitrary positive constant.

Step 2: From (22) for $k=2$, taking derivative of z_2 with respect to time yields

$$\begin{aligned}\dot{z}_2 &= \dot{x}_2 - \dot{\alpha}_{2f} \\ &= b_2x_3 + f_2 + d_2 - \dot{\alpha}_{2f}.\end{aligned} \tag{43}$$

Based on the NN approximation, it follows:

$$\begin{aligned}z_2\dot{z}_2 &= b_2z_2x_3 + z_2(f_2 + d_2 - \dot{\alpha}_{2f}) \\ &= b_2z_2\alpha_2 + \Pi_2 + \Xi_2 \\ &= b_2z_2\alpha_2 + \Pi_2 + z_2\big(W_2^{*T}S_2 + \delta_2\big)\end{aligned} \tag{44}$$

where $\Pi_2 = b_2z_2z_3 + b_2z_2y_3 + z_2f_2$ and $\Xi_2 = z_2(d_2 - \dot{\alpha}_{2f}) = z_2\Lambda_2$ with $\Lambda_2 = d_2 - \dot{\alpha}_{2f}$ being smooth function.

After applying Young inequality and Assumption 3 and implementing the similar process of (30)–(34), it can be obtained as

$$\begin{aligned}\Pi_2 + \Xi_2 &\le \varrho_{\min}\lambda_2\underline{b}_2 z_2^2\big(1 + \varphi_2^2 + 1 + \eta_{11}^2 z_1^2\big) - \varrho_{\min}\lambda_2\underline{b}_2\eta_{11}^2 z_1^2 z_2^2 \\ &\quad + \varrho_{\min}\underline{b}_3 z_2^2 z_3^2 + \varrho_{\min}\theta\underline{b}_2 S_2^2 z_2^2 + \frac{y_3^2}{4\varrho_{\min}} + \frac{\overline{b}_2^2}{4\varrho_{\min}\underline{b}_3} \\ &\quad + \frac{1}{2\varrho_{\min}\underline{b}_2} + \frac{\epsilon^2}{4\varrho_{\min}\underline{b}_2} \\ &\le \varrho_{\min}\lambda_2\underline{b}_2 z_2^2\Phi_2 - \varrho_{\min}\lambda_2\underline{b}_2\eta_{11}^2 z_1^2 z_2^2 + \varrho_{\min}\underline{b}_3 z_2^2 z_3^2 \\ &\quad + \varrho_{\min}\theta\underline{b}_2 S_2^2 z_2^2 + \frac{y_3^2}{4\varrho_{\min}} + \Delta_2\end{aligned} \tag{45}$$

where $\Phi_2 = 2 + \varphi_2^2 + \eta_{11}^2 z_1^2$ and $\Delta_2 = (\overline{b}_2^2/4\varrho_{\min}\underline{b}_3) + (1/2\varrho_{\min}\underline{b}_2) + (\epsilon^2/4\varrho_{\min}\underline{b}_2)$.

Therefore

$$z_2\dot{z}_2 \le b_2 z_2\alpha_2 + \varrho_{\min}\lambda_2\underline{b}_2 z_2^2\Phi_2 - \varrho_{\min}\lambda_2\underline{b}_2\eta_{11}^2 z_1^2 z_2^2 + \varrho_{\min}\underline{b}_3 z_2^2 z_3^2 + \varrho_{\min}\theta\underline{b}_2 S_2^2 z_2^2 + \frac{y_3^2}{4\varrho_{\min}} + \Delta_2. \quad (46)$$

The Lyapunov function is constructed as

$$V_2 = V_1 + \frac{1}{2}z_2^2 + \frac{\varrho_{\min}\underline{b}_2}{2\gamma_2}\tilde{\lambda}_2^2 + \frac{1}{2}y_3^2 \quad (47)$$

where $\gamma_2 > 0$ is the positive design parameter and $\tilde{\lambda}_2 = \lambda_2 - \hat{\lambda}_2$ is the virtual parameter estimate error.

The virtual control and adaptive control law are proposed as

$$\alpha_2 = -\left(c_2 z_2 + \hat{\lambda}_2 z_2\Phi_2 + \hat{\theta}S_2^2 z_2\right) \quad (48)$$

$$\dot{\hat{\lambda}}_2 = \gamma_2 z_2^2\Phi_2 - \mu_2\hat{\lambda}_2 \quad (49)$$

where $c_2 > 0$, $\gamma_2 > 0$, and $\mu_2 > 0$ are positive parameters to be designed.

By employing (46), (48), and (49), the time derivative of V_2 can be computed as

$$\begin{aligned}\dot{V}_2 \le{}& \dot{V}_1 + b_2 z_2\alpha_2 + \varrho_{\min}\lambda_2\underline{b}_2 z_2^2\Phi_2 - \varrho_{\min}\lambda_2\underline{b}_2\eta_{11}^2 z_1^2 z_2^2\\ &+\varrho_{\min}\underline{b}_3 z_2^2 z_3^2 + \varrho_{\min}\theta\underline{b}_2 S_2^2 z_2^2 + \frac{y_3^2}{4\varrho_{\min}} + \Delta_3\\ &-\frac{\varrho_{\min}\underline{b}_2\mu_2}{2\gamma_2}\tilde{\lambda}_2^2 + \frac{\varrho_{\min}\underline{b}_2\mu_2}{2\gamma_2}\lambda_2^2 + \left(\frac{1}{4} - \frac{1}{\tau_3}\right)y_3^2 + \Gamma_2^2\\ \le{}& -\sum_{r=1}^{2}\underline{b}_r c_r z_r^2 - \sum_{r=1}^{2}\frac{\varrho_{\min}\underline{b}_r\mu_r}{2\gamma_r}\tilde{\lambda}_r^2 - \sum_{r=1}^{2}\varepsilon_{r+1}^* y_{r+1}^2\\ &+\sum_{r=1}^{2}\varrho_{\min}\tilde{\theta}\underline{b}_r S_r^2 z_r^2 + \sum_{r=1}^{2}\omega_r + \sum_{r=1}^{2}\Gamma_r^2 + \varrho_{\min}\underline{b}_3 z_2^2 z_3^2\end{aligned} \quad (50)$$

where $-b_2 < -b_2\varrho_{\min} \le -\underline{b}_2\varrho_{\min}$, $\omega_2 = \Delta_3 + (\varrho_{\min}\underline{b}_2\mu_2)/(2\gamma_2)\lambda_2^2$, and $\varepsilon_3^* \ge (1/\tau_3) - (1/4) - (1/4\varrho_{\min})$ is the positive constant.

Step k (k = 3, ..., n-1): Similar to (28)–(35), then, it follows:

$$z_k\dot{z}_k \le z_k b_k\alpha_k + \varrho_{\min}\underline{b}_k\lambda_k z_k^2\Phi_k - \varrho_{\min}\lambda_k\underline{b}_k z_k^2 z_{k-1}^2 + \varrho_{\min}\underline{b}_{k+1} z_k^2 z_{k+1}^2 + \varrho_{\min}\theta\underline{b}_k S_k^2 z_k^2 + \frac{y_{k+1}^2}{4\varrho_{\min}} + \Delta_k \quad (51)$$

where $\Phi_k = 2 + \varphi_k^2 + z_{k-1}^2$ and $\Delta_k = (\overline{b}_k^2)/(4\varrho_{\min}\underline{b}_{k+1}) + (1/2\varrho_{\min}\underline{b}_k) + (\epsilon^2/4\varrho_{\min}\underline{b}_k)$.

Define the Lyapunov candidate function as

$$V_k = V_{k-1} + \frac{1}{2}z_k^2 + \frac{\varrho_{\min}\underline{b}_k}{2\gamma_k}\tilde{\lambda}_k^2 + \frac{1}{2}y_{k+1}^2 \quad (52)$$

where $\gamma_k > 0$ is the positive design parameter and $\tilde{\lambda}_k = \lambda_k - \hat{\lambda}_k$ is the virtual parameter estimate error.

The virtual control and adaptive controller are constructed as follows:

$$\alpha_k = -\left(c_k z_k + \hat{\lambda}_k z_k\Phi_k + \hat{\theta}S_k^2 z_k^2\right) \quad (53)$$

$$\dot{\hat{\lambda}}_k = \gamma_k z_k^2\Phi_k - \mu_k\hat{\lambda}_k. \quad (54)$$

By using (51), (53), and (54), the derivative of V_k can be obtained as

$$\begin{aligned}\dot{V}_k \le{}& \dot{V}_{k-1} - \underline{b}_k c_k z_k^2 - \frac{\varrho_{\min}\underline{b}_k\mu_k}{\gamma_k}\tilde{\lambda}_k^2 - \varepsilon_{k+1}^* y_{k+1}^2\\ &-\varrho_{\min}\lambda_k\underline{b}_k z_k^2 z_{k-1}^2 + \varrho_{\min}\underline{b}_{k+1} z_k^2 z_{k+1}^2 + \varrho_{\min}\tilde{\theta}\underline{b}_k S_k^2 z_k^2\\ &+\Gamma_k^2 + \varrho_{\min}\frac{\underline{b}_k\mu_k}{2\gamma_k}\lambda_k^2 + \Delta_k\\ \le{}& -\sum_{r=1}^{k}\underline{b}_r c_r z_r^2 - \sum_{r=1}^{k}\frac{\varrho_{\min}\underline{b}_r\mu_r}{2\gamma_r}\tilde{\lambda}_r^2 - \sum_{r=1}^{2}\varepsilon_{k+1}^* y_{k+1}^2\\ &+\sum_{r=1}^{k}\varrho_{\min}\tilde{\theta}\underline{b}_r S_r^2 z_r^2 + \sum_{r=1}^{k}\omega_r + \sum_{r=1}^{k}\Gamma_r^2 + \varrho_{\min}\underline{b}_{k+1} z_k^2 z_{k+1}^2\end{aligned} \quad (55)$$

where $-b_k < -b_k\varrho_{\min} \le -\underline{b}_k\varrho_{\min}$, $\omega_k = \Delta_k + (\varrho_{\min}\underline{b}_k\mu_k)/(2\gamma_k)\lambda_k^2$, and $\varepsilon_{k+1}^* \ge (1/\tau_{k+1}) - (1/4) - (1/4\varrho_{\min})$ is the positive constant.

Step n: From (22) for $k = n$, it follows:

$$\begin{aligned}\dot{z_n} &= \dot{x}_n - \dot{\alpha}_{nf}\\ &= b_n u + f_n + d_n - \dot{\alpha}_{nf}\\ &= b_n(\varrho u_d + \vartheta(t - t_f)\sigma_d) + f_n + d_n - \dot{\alpha}_{nf}.\end{aligned} \quad (56)$$

Applying Assumption 2, it follows:

$$\begin{aligned}z_n\dot{z_n} &= z_n(b_n u + f_n + d_n) - z_n\dot{\alpha}_{nf}\\ &= z_n b_n(\varrho u_d + \vartheta(t - t_f)\sigma_d) + \Pi_n + \Xi_n\\ &= z_n b_n(\varrho u_d + \nu_m) + \Pi_n + z_n\left(W_n^{*T}S_n + \delta_n\right)\end{aligned} \quad (57)$$

where $\Pi_n = z_n f_n$, $\Xi_n = z_n(d_n - \dot{\alpha}_{nf})$ and $\Lambda_n = d_n - \dot{\alpha}_{nf}$ with Λ_n being the smooth function.

Following the line similar to (30)–(34), it turns out:

$$\begin{aligned}&z_n b_n\nu_m + \Pi_n + \Xi_n\\ &\le \varrho_{\min}\underline{b}_n\lambda_n z_n^2\left(\varphi_n^2 + 2 + z_{n-1}^2\right) + \varrho_{\min}\underline{b}_n\theta S_n^2 z_n^2\\ &\quad-\varrho_{\min}\underline{b}_n\lambda_n z_n^2 z_{n-1}^2 + \frac{\epsilon^2}{4\varrho_{\min}\underline{b}_n} + \frac{1}{2\varrho_{\min}\underline{b}_n}\\ &\quad+\frac{1}{4\varrho_{\min}\underline{b}_n}\nu_m^2\\ &\le \varrho_{\min}\lambda_n\underline{b}_n z_n^2\Phi_n - \varrho_{\min}\lambda_n\underline{b}_n z_n^2 z_{n-1}^2\\ &\quad+\varrho_{\min}\theta\underline{b}_n S_n^2 z_n^2 + \Delta_n\end{aligned} \quad (58)$$

where $\Phi_n = \varphi_n^2 + z_{n-1}^2 + 2$ and $\Delta_n = (\epsilon^2/4\varrho_{\min}\underline{b}_n) + (1/2\varrho_{\min}\underline{b}_n) + (1/4\varrho_{\min}\underline{b}_n)\nu_m^2$.

Therefore

$$z_n\dot{z}_n \le b_n\varrho z_n u_d + \varrho_{\min}\lambda_n\underline{b}_n z_n^2\Phi_n - \varrho_{\min}\lambda_n\underline{b}_n z_n^2 z_{n-1}^2 + \varrho_{\min}\theta\underline{b}_n S_n^2 z_n^2 + \Delta_n. \quad (59)$$

The Lyapunov function is constructed as

$$V_n = V_{n-1} + \frac{1}{2}z_n^2 + \frac{\varrho_{\min}\underline{b}_n}{2\gamma_n}\tilde{\lambda}_n^2 + \frac{\varrho_{\min}\underline{b}_n}{2\beta}\tilde{\theta}^2 \quad (60)$$

where $\gamma_n > 0$ and β are positive design parameters.

The actual control and adaptive control law are designed as

$$u_d = -\left(c_n z_n + \hat{\lambda}_n z_n\Phi_n + \hat{\theta}S_n^2 z_n\right) \quad (61)$$

$$\dot{\hat{\lambda}}_n = \gamma_n z_n^2 \Phi_n - \mu_n \hat{\lambda}_n \tag{62}$$

$$\dot{\hat{\theta}} = \beta \sum_{r=1}^{n} S_r^2 z_r^2 - \kappa \hat{\theta} \tag{63}$$

with $c_n > 0, \gamma_n > 0$, and $\mu_n > 0$ assigned by designer.

According to (61)–(63), taking time derivative of V_n turns out

$$\begin{aligned}
\dot{V}_n &= \dot{V}_{n-1} + z_n \dot{z}_n - \frac{\varrho_{\min}\underline{b}_n}{\gamma_n}\tilde{\lambda}_n \dot{\hat{\lambda}}_n - \frac{\varrho_{\min}\underline{b}_n}{\beta}\tilde{\theta}\dot{\hat{\theta}} \\
&\le \dot{V}_{n-1} - \underline{b}_n c_n z_n^2 - \varrho_{\min}\lambda_n \underline{b}_n z_n^2 z_{n-1}^2 \\
&\quad - \frac{\varrho_{\min}\underline{b}_n \mu_n}{2\gamma_n}\tilde{\lambda}_n^2 + \frac{\varrho_{\min}\underline{b}_n \mu_n}{2\gamma_n}\lambda_n^2 - \frac{\varrho_{\min}\underline{b}_n \kappa}{2\beta}\tilde{\theta}^2 \\
&\quad + \frac{\varrho_{\min}\underline{b}_n \kappa}{2\beta}\theta^2 + \Delta_n \\
&\le -\sum_{r=1}^{n} \underline{b}_r c_r z_r^2 - \sum_{r=1}^{n} \frac{\varrho_{\min}\underline{b}_r \mu_r}{2\gamma_r}\tilde{\lambda}_r^2 - \sum_{r=1}^{n-1} \varepsilon_{r+1}^* y_{r+1}^2 \\
&\quad - \frac{\varrho_{\min}\underline{b}_n \kappa}{2\beta}\tilde{\theta}^2 + \sum_{r=1}^{n} \omega_r + \sum_{r=1}^{n-1} \Gamma_r^2
\end{aligned} \tag{64}$$

where $\omega_n = (\varrho_{\min}\underline{b}_b \mu_n / 2\gamma_n)\lambda_n^2 + (\varrho_{\min}\underline{b}_n \kappa / 2\beta)\theta^2 + \Delta_n$.

C. Stability Analysis

The stability analysis of manufacturing systems (1) under proposed control scheme (61)–(63) can be summarized in Theorem 1.

Theorem 1: Consider the n-order manufacturing systems (1) subject to objective function constraints (6). Suppose Assumption 1–3 hold, for any $J(0) \in \Omega$ and $(\partial J / \partial x_1) \neq 0$, if the control (61) combining with adaptive control laws (62) and (63) is applied, the following results can be obtained.

1) The asymmetric objective function constraints are never violated.
2) The feasibility conditions are completely removed.
3) All closed-loop signals are guaranteed bounded.

Proof: Define the compact sets $\Omega_d := \{[y_d, \dot{y}_d, \ddot{y}_d]^T : y_d^2 + \dot{y}_d^2 + \ddot{y}_d^2 \le Y_d\} \subset \mathbb{R}^3$ and $\Omega_j := \{[F_j, \dot{F}_j, \ddot{F}_j]^T : F_j^2 + \dot{F}_j^2 + \ddot{F}_j^2 \le F\} \subset \mathbb{R}^6$ with $j = 1, 2$ as well as $\Omega_V := \{\sum_{k=1}^n z_k^2 + \sum_{k=1}^n (b_k/\gamma_k)\tilde{\lambda}_k^2 + \sum_{k=2}^n y_k^2 + (b_n/\beta)\tilde{\theta}^2 \le 2P\} \subset \mathbb{R}^{3n}$, and then, there exists positive constant χ_i ($i = 1, \ldots, n-1$) satisfying that $|\Gamma_i| \le \chi_i$ on $\Omega_d \times \Omega_j \times \Omega_V$. From (64), it follows:

$$\begin{aligned}
\dot{V}_n &\le -\sum_{r=1}^{n} \underline{b}_r c_r z_r^2 - \sum_{r=1}^{n} \frac{\varrho_{\min}\underline{b}_r \mu_r}{2\gamma_r}\tilde{\lambda}_r^2 - \sum_{r=1}^{n-1} \varepsilon_{r+1}^* y_{r+1}^2 \\
&\quad - \frac{\varrho_{\min}\underline{b}_n \kappa}{2\beta}\tilde{\theta}^2 + \sum_{r=1}^{n} \omega_r + \sum_{r=1}^{n-1} \chi_r^2 \\
&\le -\sum_{r=1}^{n} \underline{b}_r c_r z_r^2 - \sum_{r=1}^{n} \frac{\varrho_{\min}\underline{b}_r \mu_r}{2\gamma_r}\tilde{\lambda}_r^2 - \sum_{r=1}^{n-1} \varepsilon_{r+1}^* y_{r+1}^2 \\
&\quad - \frac{\varrho_{\min}\underline{b}_n \kappa}{2\beta}\tilde{\theta}^2 + \varpi \\
&\le -\rho V_n + \varpi
\end{aligned} \tag{65}$$

where $\rho = \min\{2\underline{b}_r c_r, \mu_r, 2\varepsilon_j^*, \kappa\} > 0$ ($i = 1, \ldots, n$, $j = 2, \ldots, n$) and $\varpi = \sum_{r=1}^n \omega_r + \sum_{r=1}^{n-1} \chi_r^2 > 0$.

From (65), it can be deduced that $\dot{V}_n < 0$ on $V_n = P$ if $\rho > (\varpi / P)$. It can be verified that $V_n < P$ belongs to an invariant set, to be specific, $V_n < P$ holds if $V_n(0) \le P$ for $t \ge 0$.

By integrating both sides of (65), it yields

$$V_n \le \exp^{-\rho t} V_n(0) + \frac{\varpi}{\rho}(1 - \exp^{-\rho t}) \le V_n(0) + \frac{\varpi}{\rho}. \tag{66}$$

From the above-mentioned inequality, it is obvious that for any bounded initial condition, $V_n \in L_\infty$, which indicates that $z_i \in L_\infty$, $\tilde{\lambda}_i \in L_\infty$ for $i = 1, \ldots, n$ and $y_j \in L_\infty$ for $j = 2, \ldots, n$ as well as $\tilde{\theta} \in L_\infty$. Note that $z_1 = \zeta - \alpha_{1f}$ and α_{1f} is bounded, then ζ can be ensured bounded, which indicates from (12) that J can be bounded in constraints for any $J(0) \in \Omega$. According to the definition of J, it can be implied that x_1 is bounded. Based on $e = x_1 - y_d$, e is guaranteed bounded. From (39) and (40), it can be obtained that α_1 and $\dot{\hat{\lambda}}_1$ are bounded. Similarly, it can be inferred that $x_i, \alpha_{if}, \dot{\hat{\lambda}}_i$ ($i = 2, \ldots, n$), α_j ($j = 2, \ldots, n-1$), u, $\dot{\hat{\theta}}$ are bounded.

Reviewing the controller design process, the feasibility conditions are not attached. Therefore, it can be concluded that the feasibility conditions are removed completely.

Remark 3: In the process of control design, special treatment is applied to improve feasibility and applicability as follows.

1) A virtual parameter θ is introduced to avoid the complexity of updating weights and simplify the tedious online computation process.
2) The NN and core functions are applied to cope with uncertainties and unknown nonlinearities. For nonparametric uncertainties, the NN can be adopted to deal with. However, the core-function method is more effective for uncertainties with certain crude structural information being available. Therefore, the controller can handle various complex uncertainties gracefully.

With such treatment, the developed control scheme is simple in structure, inexpensive in computation, and undemanding in implementation.

Remark 4: Compared with those related works [6], [17], [18], the control strategy proposed in this article exhibits the following two salient features.

1) Unlike [6], [17], and [18] that only address symmetric state constraints, the proposed method is able to deal with not only asymmetric full-state constraints but also multiobjective constraints concurrently, owing to the introduction of the novel transformation function.
2) The upper constraint and lower constraint are required to be strictly positive and negative, respectively, in the aforementioned literature, whereas in the proposed method, the upper and lower bounds can be sometimes positive and sometimes negative, allowing a much larger class of constraints to be coped with.

Fig. 3. Diagram of the tire production line.

TABLE I
HEALTHY INDICATOR ϱ

Time(s)	$0 < t \leq 0.5$	$0.5 < t < 1$	$t \geq 1$
ϱ	1	0.8	$0.8 - 0.1\sin(t)$

TABLE II
UNCONTROLLABLE ADDITIVE ACTUATION FAULT

Time(s)	$0 < t \leq 2$	$t > 2$
abrupt fault	0	$0.05cos(t)$
incipient fault	0	$(1 - \exp(-2(t-2)))0.05\cos(t)$

IV. SIMULATION VERIFICATION

To validate the effectiveness of the proposed method, we conduct simulation on the conveyer belt speed control of the tire production line, as shown in Fig. 3. The model of conveyer belt system subject to multiple objective function constraints can be described as

$$\begin{aligned} M\dot{\omega} &= T - T_L \\ T &= kI \\ L\dot{I} + IR &= U \end{aligned} \tag{67}$$

where M represents the moment of inertia of the driving motor, ω denotes the angular velocity, I represents the electric current, T and T_L denote the electromagnetic torque and load torque, respectively, $k = C_t\Phi$ with C_t being torque constant and Φ being the magnetic density constant, L and R represent the inductance and the resistance in the circuit respectively, and U is the control voltage.

As voltage-driven faults and/or electromagnetic interferences in the circuit are inevitable, the driving voltage U is subject to possible failure modeled by

$$U = \varrho u_d + \sigma \tag{68}$$

where ϱ is the healthy indicator and σ is the uncontrollable additive actuation fault, which are defined in Tables I and II, respectively.

The system model of tire production line can be generalized as

$$\begin{aligned} \dot{x}_1 &= g_1 x_2 + f_1 \\ \dot{x}_2 &= g_2 u + b_2 x_2 \end{aligned} \tag{69}$$

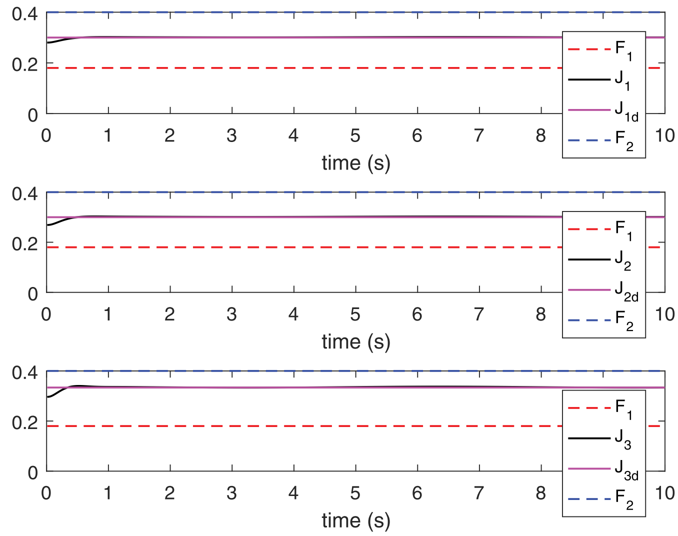

Fig. 4. Trajectories of J following J_d under different objective function constraints $J_1 = \omega_1 x_1$, $J_2 = \omega_1 x_1 + \omega_2 x_1^2$, and $J_3 = \omega_1 x_1 + \omega_2 x_1^2 + \omega_3 x_1^3$.

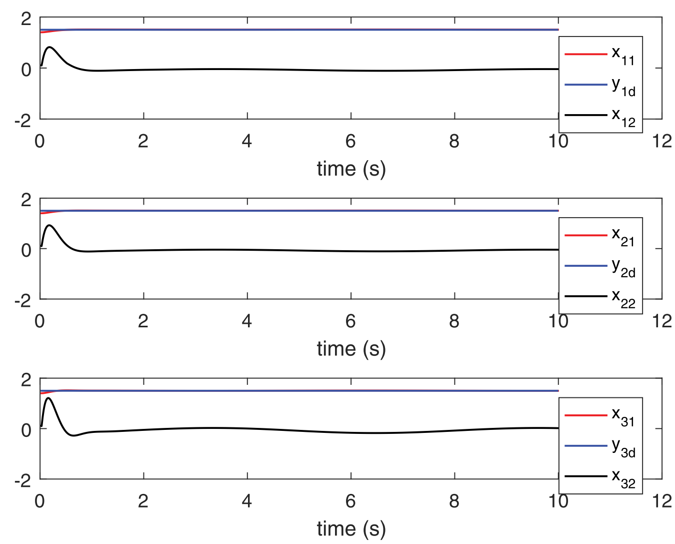

Fig. 5. States and desired trajectories under three cases.

where x_1 is the angular velocity, x_2 is the electric current, and $g_1 = (k/M)$, $f_1 = -(T_L/M)$, $g_2 = (1/L)$, $b_2 = -(R/L)$.

Note that the objective function J is bounded by

$$J \in \Omega := \{J \in \mathbb{R} : F_1(t) < J(x_1) < F_2(t)\} \tag{70}$$

where three types of objective functions are chosen as $J_1 = 0.2x_1$, $J_2 = 0.08x_1 + 0.08x_1^2$ and $J_3 = 0.08x_1 + 0.08x_1^2 + 0.01x_1^3$. J_1, J_2, and J_3 represent the state constraint, kinetic energy constraint, and special energy constraint, respectively. In order to confine these objective functions within the same constraints, the coefficient ω_i is set to be less than 1 ($\omega_1 = 1$ means that $J_1 = x_1$, which is the case with output constraints). And the constraining boundaries are set as $F_1 = 0.18$ and $F_2 = 0.4$.

The desired trajectory is set as $y_d = 1.5$, and it follows that $J_d = a_1 y_d + a_2 y_d^2 + a_3 y_d^3$. The initial values of x are set as $x(0) = [x_1(0), x_2(0)]^T = [1.4, 0.1]^T$. The control parameters

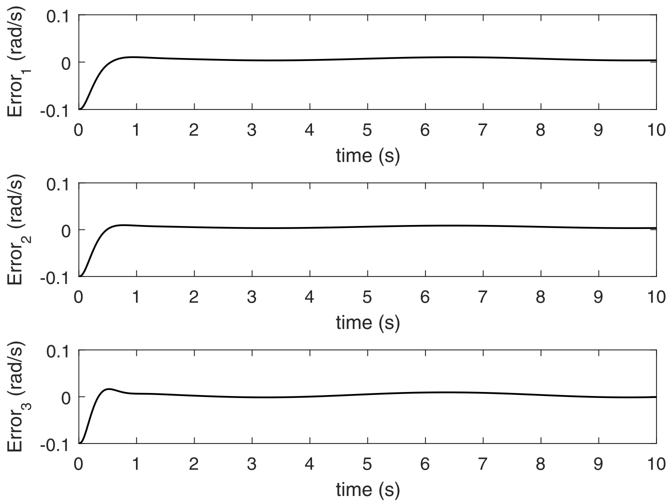

Fig. 6. Velocity tracking errors under three cases.

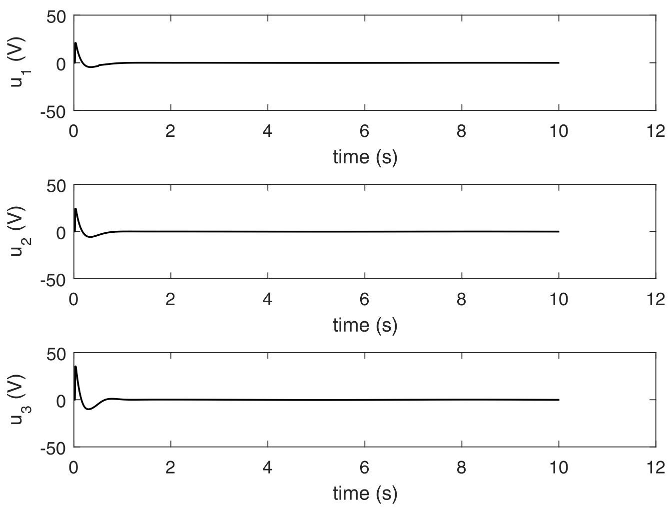

Fig. 7. Control inputs under three cases.

are given as $c_1 = 10, c_2 = 20, g_1 = 0.3, g_2 = 0.5, b_2 = -0.2, \beta = 0.01, \kappa = 0.2$, and $\tau_2 = 0.01$.

The simulation results under the three cases are depicted in Figs. 4–7, from which it is seen that with the control (61) and adaptive laws (62) and (63), the multiple objective functions are confined in prescribed constraints and closely follow the desired objective trajectories J_d as long as the initial values of objective functions satisfy the constraining conditions. From Figs. 5–7, it is observed that all closed-loop signals are continuous and bounded, confirming that the simulation results agree with the theoretical analysis.

V. CONCLUSION

This work investigated the neuroadaptive fault-tolerant control problem of process control systems in the presence of asymmetric yet time-varying multiple objective constraints and unknown disturbances. First, a novel barrier function is applied to guarantee that all objective functions are constrained in the prescribed bounds. Then, the DSC-based backstepping design procedure is carried out to derive the control algorithms, in which not only the parameter-dependent feasibility conditions are removed but also the "explosion of complexity" is avoided. Furthermore, with deep-rooted information-based approximation and NNs, the developed control strategy is simple in design, inexpensive in computation, and user-friendly in implementation. Theoretical analysis and simulation results validate that the output tracks the desired trajectory closely in the presence of objective function constraints and all closed-loop signals are ensured bounded. Two possible extensions of the proposed method are to address sensor faults/noises and to achieve practical finite-time convergence.

REFERENCES

[1] K. Zhao, Y. Song, and C. Wen, "Computationally inexpensive fault tolerant control of uncertain non-linear systems with non-smooth asymmetric input saturation and undetectable actuation failures," *IET Control Theory Appl.*, vol. 10, no. 15, pp. 1866–1873, Oct. 2016.

[2] C. Wang, "Semiglobal practical stabilization of nonholonomic wheeled mobile robots with saturated inputs," *Automatica*, vol. 44, no. 3, pp. 816–822, Mar. 2008.

[3] A. Pervozvanski and L. Freidovich, "Robust stabilization of robotic manipulators by PID controllers," *Dyn. Control*, vol. 9, no. 3, pp. 203–222, Jul. 1999.

[4] K. Zhao, Y. Song, T. Ma, and L. He, "Prescribed performance control of uncertain Euler–Lagrange systems subject to full-state constraints," *IEEE Trans. Neural Netw. Learn. Syst.*, vol. 29, no. 8, pp. 3478–3489, Aug. 2018.

[5] A. Shiriaev, L. Freidovich, and S. Gusev, "Transverse linearization for controlled mechanical systems with several passive degrees of freedom," *IEEE Trans. Autom. Control.*, vol. 55, no. 4, pp. 893–906, Apr. 2010.

[6] W. He, Y. Chen, and Z. Yin, "Adaptive neural network control of an uncertain robot with full-state constraints," *IEEE Trans. Cybern.*, vol. 46, no. 3, pp. 620–629, Mar. 2016.

[7] B. Ren, S. Sam Ge, K. Peng Tee, and T. Heng Lee, "Adaptive neural control for output feedback nonlinear systems using a barrier Lyapunov function," *IEEE Trans. Neural Netw.*, vol. 21, no. 8, pp. 1339–1345, Aug. 2010.

[8] K. Zhao, Y. Song, and Z. Shen, "Neuroadaptive fault-tolerant control of nonlinear systems under output constraints and actuation faults," *IEEE Trans. Neural Netw. Learn. Syst.*, vol. 29, no. 2, pp. 286–298, Feb. 2018.

[9] K. P. Tee, S. S. Ge, and E. H. Tay, "Barrier Lyapunov functions for the control of output-constrained nonlinear systems," *Automatica*, vol. 45, no. 4, pp. 918–927, Apr. 2009.

[10] J. Liu and K. Xie, "Emergency materials transportation model in disasters based on dynamic programming and ant colony optimization," *Kybernetes*, vol. 46, no. 4, pp. 656–671, Apr. 2017.

[11] J. Branke, B. Scheckenbach, M. Stein, K. Deb, and H. Schmeck, "Portfolio optimization with an envelope-based multi-objective evolutionary algorithm," *Eur. J. Oper. Res.*, vol. 199, no. 3, pp. 684–693, Dec. 2009.

[12] J. S. Chung and S. M. Hwang, "Process optimal design in forging by genetic algorithm," *J. Manuf. Sci. Eng.*, vol. 124, no. 2, pp. 397–408, May 2002.

[13] D. Mayne, J. Rawlings, C. Rao, and P. Scokaert, "Constrained model predictive control: Stability and optimality," *Automatica*, vol. 36, no. 6, pp. 789–814, Jun. 2000.

[14] A. Bemporad, "Reference governor for constrained nonlinear systems," *IEEE Trans. Autom. Control.*, vol. 43, no. 3, pp. 415–419, Mar. 1998.

[15] D. Dehaan and M. Guay, "Extremum-seeking control of state-constrained nonlinear systems," *IFAC Proc. Volumes*, vol. 37, no. 13, pp. 663–668, Sep. 2004.

[16] Y.-J. Liu, D.-J. Li, and S. Tong, "Adaptive output feedback control for a class of nonlinear systems with full-state constraints," *Int. J. Control*, vol. 87, no. 2, pp. 281–290, Feb. 2014.

[17] Y.-J. Liu and S. Tong, "Barrier Lyapunov functions-based adaptive control for a class of nonlinear pure-feedback systems with full state constraints," *Automatica*, vol. 64, pp. 70–75, Feb. 2016.

[18] Y.-J. Liu and S. Tong, "Barrier Lyapunov functions for Nussbaum gain adaptive control of full state constrained nonlinear systems," *Automatica*, vol. 76, pp. 143–152, Feb. 2017.

[19] K. P. Tee and S. S. Ge, "Control of nonlinear systems with partial state constraints using a barrier Lyapunov function," *Int. J. Control*, vol. 84, no. 12, pp. 2008–2023, Dec. 2011.

[20] Z.-L. Tang, S. S. Ge, K. P. Tee, and W. He, "Robust adaptive neural tracking control for a class of perturbed uncertain nonlinear systems with state constraints," *IEEE Trans. Syst. Man Cybern, Syst.*, vol. 46, no. 12, pp. 1618–1629, Dec. 2016.

[21] Y.-J. Liu, S. Tong, C. L. P. Chen, and D.-J. Li, "Adaptive NN control using integral barrier Lyapunov functionals for uncertain nonlinear block-triangular constraint systems," *IEEE Trans. Cybern.*, vol. 47, no. 11, pp. 3747–3757, Nov. 2017.

[22] D.-P. Li, Y.-J. Liu, S. Tong, C. L. P. Chen, and D.-J. Li, "Neural networks-based adaptive control for nonlinear state constrained systems with input delay," *IEEE Trans. Cybern.*, vol. 49, no. 4, pp. 1249–1258, Apr. 2019.

[23] D. Hardt, B. Anthony, and S. Tor, "A teaching factory for polymer microfabrication—μFac," *Int. J. Nanomanufacturing*, vol. 6, nos. 1–4, pp. 137–151, Aug. 2010.

[24] E. M. B. Aske, S. Strand, and S. Skogestad, "Coordinator MPC for maximizing plant throughput," *Comput. Chem. Eng.*, vol. 32, nos. 1–2, pp. 195–204, Jan. 2008.

[25] B. Liu, Q. Sun, and A. El Kamel, "Improving the intersection's throughput using V2X communication and cooperative adaptive cruise control," *IFAC-PapersOnLine*, vol. 49, no. 5, pp. 359–364, 2016.

[26] S.-J. Chuu, "Evaluating the flexibility in a manufacturing system using fuzzy multi-attribute group decision-making with multi-granularity linguistic information," *Int. J. Adv. Manuf. Technol.*, vol. 32, nos. 3–4, pp. 409–421, Feb. 2007.

[27] F. T. S. Chan, K. C. Au, L. Y. Chan, T. L. Lau, and K. L. Choy, "A genetic algorithm approach to machine flexibility problems in an ion plating cell," *Int. J. Adv. Manuf. Technol.*, vol. 31, nos. 11–12, pp. 1127–1134, Jan. 2007.

[28] H.-S. Park, T.-T. Nguyen, and X.-P. Dang, "Multi-objective optimization of turning process of hardened material for energy efficiency," *Int. J. Precis. Eng. Manuf.*, vol. 17, no. 12, pp. 1623–1631, Dec. 2016.

[29] L. Zhou, J. Li, F. Li, Q. Meng, J. Li, and X. Xu, "Energy consumption model and energy efficiency of machine tools: A comprehensive literature review," *J. Cleaner Prod.*, vol. 112, pp. 3721–3734, Jan. 2016.

[30] W. Meng, Q. Yang, and Y. Sun, "Adaptive neural control of nonlinear MIMO systems with time-varying output constraints," *IEEE Trans. Neural Netw. Learn. Syst.*, vol. 26, no. 5, pp. 1074–1085, May 2015.

[31] T. Zhang, H. Liu, M. Xia, and Y. Yi, "Adaptive neural control of MIMO uncertain nonlinear systems with unmodeled dynamics and output constraint," *Int. J. Adapt. Control Signal Process.*, vol. 32, no. 12, pp. 1731–1747, Dec. 2018.

[32] X. Jin, "Fault tolerant nonrepetitive trajectory tracking for MIMO output constrained nonlinear systems using iterative learning control," *IEEE Trans. Cybern.*, vol. 49, no. 8, pp. 3180–3190, Aug. 2019.

[33] K. Zhao and Y. Song, "Removing the feasibility conditions imposed on tracking control designs for state-constrained strict-feedback systems," *IEEE Trans. Autom. Control.*, vol. 64, no. 3, pp. 1265–1272, Mar. 2019.

[34] Y. Li, Z. Ma, and S. Tong, "Adaptive fuzzy fault-tolerant control of nontriangular structure nonlinear systems with error constraint," *IEEE Trans. Fuzzy Syst.*, vol. 26, no. 4, pp. 2062–2074, Aug. 2018.

[35] M. Polycarpou and P. Ioannou, "A robust adaptive nonlinear control design," *Automatica*, vol. 32, no. 3, pp. 423–427, Mar. 1996.

[36] Y.-J. Liu, S. Li, S. Tong, and C. L. P. Chen, "Adaptive reinforcement learning control based on neural approximation for nonlinear discrete-time systems with unknown nonaffine dead-zone input," *IEEE Trans. Neural Netw. Learn. Syst.*, vol. 30, no. 1, pp. 295–305, Jan. 2019.

[37] Y. Song and J. Guo, "Neuro-adaptive fault-tolerant tracking control of Lagrange systems pursuing targets with unknown trajectory," *IEEE Trans. Ind. Electron.*, vol. 64, no. 5, pp. 3913–3920, May 2017.

[38] K. Zhao and Y. Song, "Neuroadaptive robotic control under time-varying asymmetric motion constraints: A feasibility-condition-free approach," *IEEE Trans. Cybern.*, vol. 50, no. 1, pp. 15–24, Jan. 2020.

[39] W. Chen, S. S. Ge, J. Wu, and M. Gong, "Globally stable adaptive backstepping neural network control for uncertain strict-feedback systems with tracking accuracy known a Priori," *IEEE Trans. Neural Netw. Learn. Syst.*, vol. 26, no. 9, pp. 1842–1854, Sep. 2015.

[40] R. Sanner and J. Slotine, "Gaussian networks for direct adaptive control," *IEEE Trans. Neural Netw.*, vol. 3, no. 6, pp. 837–863, Nov. 1992.

[41] J. Park and I. W. Sandberg, "Universal approximation using radial-basis-function networks," *Neural Comput.*, vol. 3, no. 2, pp. 246–257, Jun. 1991.

[42] K. Zhao and J. Chen, "Adaptive neural quantized control of MIMO nonlinear systems under actuation faults and time-varying output constraints," *IEEE Trans. Neural Netw. Learn. Syst.*, early access, doi: 10.1109/TNNLS.2019.2944690.

[43] A. J. Calise, N. Hovakimyan, and M. Idan, "Adaptive output feedback control of nonlinear systems using neural networks," *Automatica*, vol. 37, no. 8, pp. 1201–1211, Aug. 2001.

Qian Cui received the B.S. degree from the Wuhan Institute of Technology, Wuhan, China, in 2017. She is currently pursuing the Ph.D. degree with the School of Automation, Chongqing University, Chongqing, China.

Her research interests include robust adaptive control, neural networks, and learning systems.

Yujuan Wang received the Ph.D. degree in control theory and control engineering from Chongqing University, Chongqing, China, in 2016.

She is currently an Associate Professor with the School of Automation, Chongqing University. Her research interests include distributed control, adaptive control, finite-time control, and fault-tolerant control.

Yongduan Song (Fellow, IEEE) received the Ph.D. degree in electrical and computer engineering from Tennessee Technological University, Cookeville, TN, USA, in 1992.

He was a tenured Full Professor with North Carolina A&T State University, Greensboro, NC, USA, from 1993 to 2008, and a Langley Distinguished Professor with the National Institute of Aerospace, Hampton, VA, USA, from 2005 to 2008. He is currently the Dean of the School of Automation, Chongqing University, Chongqing, China. He was the Founding Director of the Cooperative Systems with NIA. His current research interests include intelligent systems, guidance navigation and control, and bioinspired adaptive and cooperative systems.

Dr. Song was a recipient of several competitive research awards from the National Science Foundation, the National Aeronautics and Space Administration, the U.S. Air Force Office, the U.S. Army Research Office, and the U.S. Naval Research Office. He has served/has been serving as an Associate Editor for several prestigious international journals, including the IEEE TRANSACTIONS ON AUTOMATIC CONTROL, the IEEE TRANSACTIONS ON NEURAL NETWORKS AND LEARNING SYSTEMS, the IEEE TRANSACTIONS ON INTELLIGENT TRANSPORTATION SYSTEMS, the IEEE TRANSACTIONS ON SYSTEMS, MAN, AND CYBERNETICS, and the IEEE TRANSACTIONS ON DEVELOPMENTAL AND COGNITIVE SYSTEMS.